

# 1D Helix, 2D Brick-Wall and Herringbone, and 3D Interpenetration d<sup>10</sup> Metal–Organic Framework Structures Assembled from Pyridine-2,6-dicarboxylic Acid *N*-Oxide

Li-Li Wen, Dong-Bin Dang, Chun-Ying Duan, Yi-Zhi Li, Zheng-Fang Tian, and Qing-Jin Meng\*

Coordination Chemistry Institute, State Key Laboratory of Coordination Chemistry, Nanjing University, Nanjing 210093, P.R. China

Received June 18, 2005

Five novel interesting d<sup>10</sup> metal coordination polymers, [Zn(PDCO)(H<sub>2</sub>O)<sub>2</sub>]<sub>n</sub> (PDCO = pyridine-2,6-dicarboxylic acid *N*-oxide) (**1**), [Zn<sub>2</sub>(PDCO)<sub>2</sub>(4,4'-bpy)<sub>2</sub>(H<sub>2</sub>O)<sub>2</sub>·3H<sub>2</sub>O]<sub>n</sub> (bpy = bipyridine) (**2**), [Zn(PDCO)(bix)]<sub>n</sub> (bix = 1,4-bis(imidazol-1-ylmethyl)benzene) (**3**), [Zn(PDCO)(bbi)·0.5H<sub>2</sub>O]<sub>n</sub> (bbi = 1,1'-(1,4-butanediyl)bis(imidazole)) (**4**), and [Cd(PDCO)(bix)<sub>1.5</sub>·1.5H<sub>2</sub>O]<sub>n</sub> (**5**), have been synthesized under hydrothermal conditions and structurally characterized. Polymer **1** possesses a one-dimensional (1D) helical chainlike structure with 4<sub>1</sub> helices running along the *c*-axis with a pitch of 10.090 Å. Polymer **2** has an infinite chiral two-dimensional (2D) brick-wall-like layer structure in the *ac* plane built from achiral components, while both **3** and **4** exhibit an infinite 2D herringbone architecture, respectively extended in the *ac* and *ab* plane. Polymer **5** features a most remarkable and unique three-dimensional (3D) porous framework with 2-fold interpenetration related by symmetry, which contains channels in the *b* and *c* directions, both distributed in a rectangular grid fashion. Compounds **1**–**5**, with systematic variation in dimensionality from 1D to 2D to 3D, are the first examples of d<sup>10</sup> metal coordination polymers into which pyridinedicarboxylic acid *N*-oxide has been introduced. In addition, polymers **1**, **4**, and **5** display strong blue fluorescent emissions in the solid state. Polymer **3** exhibits a strong SHG response, estimated to be approximately 0.9 times that of urea.

## Introduction

The rational design of novel metal–organic frameworks (MOFs) has attracted great interest from chemists in recent years,<sup>1,2</sup> and considerable efforts have been focused on the design synthesis and characterization of novel multidimensional not only because of their intriguing variety of architectures and topologies but also because of their fascinating potential applications in functional solid materials,

ion exchange, catalysis, and the development of optical, electronic, and magnetic devices.<sup>4,5</sup>

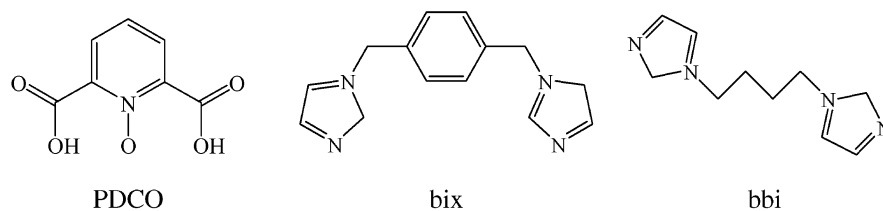
The MOFs are essentially assembled by very strong and highly directional coordinative interactions between metal centers and multitopic organic ligands, thus combining properties of both purely organic and inorganic compounds.<sup>6</sup> The multidentate O-donor organic aromatic polycarboxylate ligands, such as 1,4-benzenedicarboxylate, 1,3,5-benzene-

\* To whom correspondence should be addressed. E-mail: mengqj@nju.edu.cn. Phone: +86 25 83597266. Fax: +86 25 83314502.

- (1) Janiak, C. *Angew. Chem., Int. Ed. Engl.* **1997**, *36*, 1431. Batten, S. R.; Robson, R. *Angew. Chem., Int. Ed.* **1998**, *37*, 1461. Moulton, B.; Zaworotko, M. J. *Chem. Rev.* **2001**, *101*, 1629. Zaworotko, M. J. *Chem. Commun.* **2001**, 1. Janiak, C. *J. Chem. Soc., Dalton Trans.* **2003**, 2781. Carlucci, L.; Ciani, G.; Proserpio, D. M. *Coord. Chem. Rev.* **2003**, *246*, 247.
- (2) Lehn, J. M. *Supramolecular Chemistry: Concepts and Perspectives*; VCH: New York, 1995. Steed, J. W.; Atwood, J. L. *Supramolecular Chemistry*; Wiley and Sons: New York, 2000. Bond, A. D.; Jones, W. In *Supramolecular Organization and Materials Design*; Jones, W., Rao, C. N. R., Eds.; Cambridge University Press: Cambridge, U.K., 2002. Desiraju, G. R. *Crystal Design: Structure and Function*; Perspectives in Supramolecular Chemistry Vol. 6; Wiley: Chichester, U.K., 2003.

- (3) Eddaoudi, M.; Moler, D. B.; Li, H. L.; Chen, B. L.; Reineke, T. M.; O'Keeffe, M.; Yaghi, O. M. *Acc. Chem. Res.* **2001**, *34*, 319. James, S. L. *Chem. Soc. Rev.* **2003**, *32*, 276. Kitagawa, S.; Kitaura, R.; Noro, S.-i. *Angew. Chem., Int. Ed.* **2004**, *43*, 2334. Khlobystov, A. N.; Blake, A. J.; Champness, N. R.; Lemenovskii, D. A.; Majouga, A. G.; Zyk, N. V.; Schroder, M. *Coord. Chem. Rev.* **2001**, *222*, 155.
- (4) Moulton, B.; Zaworotko, M. J. *Chem. Rev.* **2001**, *101*, 1629. Zaworotko, M. J. *Chem. Commun.* **2001**, 1.
- (5) Hagrman, P. J.; Hagrman, D.; Zubieta, J. *Angew. Chem., Int. Ed.* **1999**, *38*, 2638. Ma, B. Q.; Gao, S.; Su, G.; Xu, G. X. *Angew. Chem., Int. Ed.* **2001**, *40*, 434. Yeung, W. F.; Man, W. L.; Wong, W. Y.; Lau, T. C.; Gao, S. *Angew. Chem., Int. Ed.* **2001**, *40*, 3031. Inoue, K.; Imai, H.; Ghalsasi, P. S.; Kikuchi, K.; Ohba, M.; Okawa, H.; Yakhmi, J. V. *Angew. Chem., Int. Ed.* **2001**, *40*, 4242.
- (6) Coe, S.; Kane, J. J.; Nguyen, T. L.; Toledo, L. M.; Winger, E.; Fowler, F. W.; Lauher, J. W. *J. Am. Chem. Soc.* **1997**, *119*, 86. Braga, D.; Angeloni, A.; Maini, L.; Gotz, A. W.; Grepioni, F. *New J. Chem.* **1999**, *23*, 17.

Chart 1



tricarboxylate, and 1,2,4,5-benzenetetracarboxylate, have been extensively employed in the construction of a rich variety of high-dimensional structures.<sup>7,8</sup> However, pyridine-2,6-dicarboxylic acid *N*-oxide (PDCO) (Chart 1), which has limited steric hindrance and weak stacking interactions and can offer possibilities to form coordination polymers through a carboxylate and *N*-oxide bridge, remains largely unexplored. To the best of our knowledge, there has been only one reported polymer based on the PDCO ligand hitherto.<sup>9</sup> The *N*-oxide group of PDCO is a far better electron donor than the ring nitrogen atom of pyridine-2,6-dicarboxylic acid.<sup>10</sup> Therefore, with the aim of preparing novel materials with beautiful architecture and excellent physical properties, we start to elaborate new high-dimensional coordination polymers constructed from pyridine-2,6-dicarboxylic acid *N*-oxide, with the introduction of N-containing auxiliary ligands, such as rigid pyridyl-based 4,4'-bpy<sup>11</sup> and highly flexible imidazole-based bix and bbi (Chart 1),<sup>12,13</sup> into {M–PDCO} (M = Zn<sup>2+</sup>, Cd<sup>2+</sup>), which afford the new structures and fine-tune the structural motif of these MOFs. In this paper, we report five interesting coordination polymeric complexes [Zn(PDCO)(H<sub>2</sub>O)<sub>2</sub>]<sub>n</sub> (**1**), [Zn<sub>2</sub>(PDCO)<sub>2</sub>(4,4'-bpy)<sub>2</sub>(H<sub>2</sub>O)<sub>2</sub>·3H<sub>2</sub>O]<sub>n</sub> (**2**), [Zn(PDCO)(bix)]<sub>n</sub> (**3**), [Zn(PDCO)(bbi)·0.5H<sub>2</sub>O]<sub>n</sub> (**4**), and [Cd(PDCO)(bix)<sub>1.5</sub>·1.5H<sub>2</sub>O]<sub>n</sub> (**5**). These MOFs have several unusual features: (i) They are the first examples of d<sup>10</sup> metal coordination polymers into which pyridine dicarboxylic acid *N*-oxide has been introduced. (ii) d<sup>10</sup> center metals and the conjugated  $\pi$  systems containing aromatic rings favor the development of fluorescent materials.<sup>14,15</sup> (iii) Compounds **1–3** are absent of a

center of symmetry, which meets the essential requirement of a second harmonic generation (SHG) response.<sup>16</sup> **3** exhibits a strong SHG response relative to urea; thus, it can be used to form novel hybrid inorganic–organic NLO materials which are currently investigated widely due to their possible applications in optical switching, optical data processing, image processing, etc.<sup>17,18</sup>

## Experimental Section

**Materials and Measurements.** The reagents and solvents employed were commercially available and used as received without further purification. PDCO, bix, and bbi were synthesized as reported previously.<sup>19–21</sup> The C, H, and N microanalyses were carried out with a Perkin-Elmer 240 elemental analyzer. The IR spectra were recorded on KBr disks on a Bruker Vector 22 spectrophotometer in the 4000–400 cm<sup>-1</sup> region. Luminescence spectra for the solid samples were recorded with a Hitachi 850 fluorescence spectrophotometer. Thermogravimetric analyses were performed on a simultaneous SDT 2960 thermal analyzer under flowing N<sub>2</sub> with a heating rate of 10 °C/min between ambient temperature and 800 °C. Powder X-ray diffraction patterns were recorded on a RigakuD/max-RA rotating anode X-ray diffractometer with graphite monochromatic Cu K $\alpha$  ( $\lambda$  = 1.542 Å) radiation at room temperature. A pulsed Q-switched Nd:YAG laser at a wavelength of 1064 nm was used to generate an SHG signal from samples. The backward scattered SHG light was collected using a spherical concave mirror and passed through a filter which transmits only 532 nm radiation.

**Hydrothermal Syntheses.** [Zn(PDCO)(H<sub>2</sub>O)<sub>2</sub>]<sub>n</sub> (**1**). A mixture of Zn(NO<sub>3</sub>)<sub>2</sub>·6H<sub>2</sub>O (0.6 mmol), PDCO (0.6 mmol), triethylamine (1.2 mmol), and H<sub>2</sub>O (4 mL) was placed in a Parr Teflon-lined stainless steel vessel (25 cm<sup>3</sup>), and then the vessel was sealed and heated at 120 °C for 3 days. After the mixture was slowly cooled to room temperature, colorless crystals of **1** were obtained (yield: 84% based on Zn). Anal. Calcd for C<sub>7</sub>H<sub>7</sub>NO<sub>7</sub>Zn: C, 29.76; H, 2.50; N, 4.96. Found: C, 29.72; H, 2.55; N, 5.01. IR spectrum (cm<sup>-1</sup>): 3386 (s), 3181 (s), 1672 (s), 1625 (s), 1477 (m), 1408 (s), 1359 (s), 1247 (s), 1197 (s), 1168 (w), 1091 (w), 1008 (w), 913 (m), 857 (m), 776 (s), 735 (m), 720 (m), 630 (m), 598 (m), 532 (m), 485 (m), 429 (w).

[Zn<sub>2</sub>(PDCO)<sub>2</sub>(4,4'-bpy)<sub>2</sub>(H<sub>2</sub>O)<sub>2</sub>·3H<sub>2</sub>O]<sub>n</sub> (**2**). A mixture of Zn(NO<sub>3</sub>)<sub>2</sub>·6H<sub>2</sub>O (0.6 mmol), PDCO (0.6 mmol), 4,4'-bpy (0.6 mmol),

- (7) Li, H.; Eddaoudi, M.; O'Keeffe, M.; Yaghi, O. M. *Nature* **1999**, *402*, 276. Chui, S. S.-Y.; Lo, S. M.-F.; Charmant, J. P. H.; Orpen, A. G.; Williams, I. D. *Science* **1999**, *283*, 1148. Kim, J.; Chen, B.; Reineke, T. M.; Li, H.; Eddaoudi, M.; Moler, D. B.; O'Keeffe, M.; Yaghi, O. M. *J. Am. Chem. Soc.* **2001**, *123*, 8239. Rosi, N. L.; Eckert, J.; Eddaoudi, M.; Vodak, D. T.; Kim, J.; O'Keeffe, M.; Yaghi, O. M. *Science* **2003**, *300*, 1127.
- (8) Barthelet, K.; Marrot, J.; Riou, D.; Férey, G. *Angew. Chem., Int. Ed.* **2002**, *41*, 281. Millange, F.; Serre, C.; Férey, G. *Chem. Commun.* **2002**, 822. Dybtsev, D. N.; Chun, H.; Kim, K. *Angew. Chem., Int. Ed.* **2004**, *43*, 5033.
- (9) Nathan, L. C.; Doyle, C. A.; Mooring, A. M.; Zapfen, D. C.; Larsen, S. K.; Pierpont, C. G. *Inorg. Chem.* **1985**, *24*, 2763.
- (10) Paul, D. B. *Aust. J. Chem.* **1984**, *37*, 87.
- (11) Carlucci, L.; Ciani, G.; Proserpio, D. M. *Chem. Commun.* **2004**, 380.
- (12) Hoskins, B. F.; Robson, R.; Slizys, D. A. *Angew. Chem., Int. Ed. Engl.* **1997**, *36*, 2336.
- (13) Duncan, P. C. M.; Goodgame, D. M. L.; Menzer, S.; Williams, D. J. *Chem. Commun.* **1996**, 2127. Ma, J. F.; Liu, J. F.; Xing, Y.; Jia, H. Q.; Lin, Y. H. *J. Chem. Soc., Dalton Trans.* **2000**, 2403.
- (14) Tong, M. L.; Chen, X. M.; Ye, B. H.; Ji, L. N. *Angew. Chem., Int. Ed.* **1999**, *38*, 2237.
- (15) Grummt, U. W.; Birckner, E.; Klemm, E.; Egbe, D. A. M.; Heise, B. *J. Phys. Org. Chem.* **2000**, *13*, 112. Zhang, X. M.; Tong, M. L.; Gong, M. L.; Chen, X. M. *Eur. J. Inorg. Chem.* **2003**, 138. Wang, X. L.; Qin, C.; Wang, E. B.; Xu, L.; Su, Z. M.; Hu, C. W. *Angew. Chem., Int. Ed.* **2004**, *43*, 5036.

- (16) Zyss, J. *Molecular Nonlinear Optics: Material, Physics, and Devices*; Academic Press: New York, 1993. Newnhan, R. E. *Structure–Property Relationships*; Springer: New York, 1975.
- (17) Xiong, R. G.; Zuo, J. L.; You, X. Z.; Abrahams, B. F.; Bai, Z. P.; Che, C. M.; Fun, H. K. *Chem. Commun.* **2000**, 2061. Bella, S. D. *Chem. Soc. Rev.* **2001**, *30*, 355.
- (18) Karna, S. P.; Yeates, A. T. *Nonlinear Optical Materials*; American Chemical Society: Washington, DC, 1996.
- (19) Heywood, D. L.; Dunn, J. T. *J. Org. Chem.* **1959**, *24*, 1569.
- (20) Hoskins, B. F.; Robson, R.; Slizys, D. A. *J. Am. Chem. Soc.* **1997**, *119*, 2952.
- (21) Ballester, L.; Baxter, I.; Duncan, P. C. M.; Goodgame, D. M. L.; Grachvogel, D. A.; Williams, D. J. *Polyhedron* **1998**, *17*, 3613.

**Table 1.** Crystal Data and Structure Refinement Information for Compounds 1–5

param	1	2	3	4	5
empirical formula	C <sub>7</sub> H <sub>7</sub> NO <sub>7</sub> Zn	C <sub>34</sub> H <sub>32</sub> N <sub>6</sub> O <sub>15</sub> Zn <sub>2</sub>	C <sub>21</sub> H <sub>17</sub> N <sub>5</sub> O <sub>5</sub> Zn	C <sub>68</sub> H <sub>72</sub> N <sub>20</sub> O <sub>22</sub> Zn <sub>4</sub>	C <sub>112</sub> H <sub>108</sub> Cd <sub>4</sub> N <sub>28</sub> O <sub>26</sub>
fw	282.51	895.40	484.77	1782.94	2711.86
cryst syst	tetragonal	monoclinic	orthorhombic	orthorhombic	monoclinic
space group	<i>I</i> <sub>4</sub> <i>cd</i>	<i>P</i> 2 <sub>1</sub>	<i>Pca</i> 2 <sub>1</sub>	<i>Pbca</i>	<i>P</i> 2 <sub>1</sub> <i>c</i>
<i>a</i> (Å)	16.675(3)	10.825(2)	20.740(2)	12.807(3)	16.457(4)
<i>b</i> (Å)	16.675(3)	16.860(3)	8.441(1)	16.145(4)	9.193(2)
<i>c</i> (Å)	13.222(3)	11.004(2)	11.486(1)	17.415(4)	21.244(4)
$\beta$ (deg)	90.00	99.03(3)	90.00	90.00	113.52(1)
<i>V</i> (Å <sup>3</sup> )	3676.6(11)	1983.4(7)	2011.0(4)	3600.7(15)	2946.9(11)
<i>Z</i>	16	2	4	2	1
abs coeff (mm <sup>-1</sup> )	2.695	1.284	1.268	1.409	0.796
<i>F</i> (000)	2272	916	992	1832	1376
limiting indices	−20 ≤ <i>h</i> ≤ 20 −20 ≤ <i>k</i> ≤ 12 −15 ≤ <i>l</i> ≤ 16	−13 ≤ <i>h</i> ≤ 13 −20 ≤ <i>k</i> ≤ 20 −13 ≤ <i>l</i> ≤ 13	−26 ≤ <i>h</i> ≤ 23 −10 ≤ <i>k</i> ≤ 9 −14 ≤ <i>l</i> ≤ 14	−13 ≤ <i>h</i> ≤ 15 −12 ≤ <i>k</i> ≤ 19 −20 ≤ <i>l</i> ≤ 20	−20 ≤ <i>h</i> ≤ 20 −11 ≤ <i>k</i> ≤ 11 −26 ≤ <i>l</i> ≤ 20
reflens colld	1786	7765	4338	3169	5767
indep reflens	1644	6731	3731	2362	3777
GOF on <i>F</i> <sup>2</sup>	1.043	1.029	1.054	0.976	0.986
<i>R</i> <sub>1</sub> [ <i>I</i> > 2σ( <i>I</i> )]	0.0589	0.0426	0.0500	0.0467	0.0484
w <i>R</i> <sub>2</sub>	0.1468	0.0929	0.1026	0.0928	0.0885

NaOH (1.2 mmol), and H<sub>2</sub>O (5 mL) was heated at 120 °C for 3 days in a procedure analogous to that for **1**. After the reactant mixture was slowly cooled to room temperature, colorless crystals of **2** were obtained (yield: 65% based on Zn). Anal. Calcd for C<sub>34</sub>H<sub>32</sub>N<sub>6</sub>O<sub>15</sub>Zn<sub>2</sub>: C, 45.61; H, 3.60; N, 9.39. Found: C, 45.70; H, 3.68; N, 9.43. IR spectrum (cm<sup>-1</sup>): 3425 (m), 1612 (s), 1535 (w), 1489 (w), 1415 (m), 1384 (s), 1216 (m), 1071 (m), 1046 (w), 1015 (w), 860 (s), 808 (s), 774 (m), 727 (w), 705 (w), 674 (w), 642 (m), 609 (w), 570 (w), 493 (w), 465 (w).

[Zn(PDCO)(bix)]<sub>n</sub> (**3**). The synthesis was similar to that described for **2** except using bix (0.6 mmol) instead of 4,4'-bpy, and colorless crystals of **3** were obtained (yield: 54% based on Zn). Anal. Calcd for C<sub>21</sub>H<sub>17</sub>N<sub>5</sub>O<sub>5</sub>Zn: C, 52.03; H, 3.53; N, 14.45. Found: C, 52.06; H, 3.62; N, 14.51. IR spectrum (cm<sup>-1</sup>): 3423 (m), 3111 (s), 1654 (m), 1640 (s), 1595 (m), 1531 (m), 1520 (m), 1444 (m), 1394 (s), 1368 (m), 1339 (s), 1253 (w), 1234 (m), 1190 (m), 1110 (s), 1092 (s), 957 (m), 898 (m), 847 (m), 811 (m), 795 (w), 766 (m), 757 (m), 732 (m), 707 (s), 659 (s), 624 (m), 595 (m), 535 (w), 516 (w), 483 (w), 452 (w).

[Zn(PDCO)(bbi)·0.5H<sub>2</sub>O]<sub>n</sub> (**4**). The synthesis was similar to that described for **2** except using bbi (0.6 mmol) instead of 4,4'-bpy, and colorless crystals of **4** were obtained (yield: 62% based on Zn). Anal. Calcd for C<sub>68</sub>H<sub>72</sub>N<sub>20</sub>O<sub>22</sub>Zn<sub>4</sub>: C, 45.81; H, 4.07; N, 15.71. Found: C, 45.76; H, 4.14; N, 15.62. IR spectrum (cm<sup>-1</sup>): 3419 (m), 3129 (s), 1650 (s), 1592 (m), 1528 (m), 1466 (w), 1390 (s), 1372 (s), 1331 (s), 1276 (m), 1247 (m), 1210 (m), 1177 (w), 1101 (s), 949 (m), 903 (w), 851 (s), 785 (s), 764 (w), 735 (w), 709 (s), 661 (m), 622 (w), 595 (w), 527 (w), 453 (w).

[Cd(PDCO)(bix)<sub>1.5</sub>·1.5H<sub>2</sub>O]<sub>n</sub> (**5**). The synthesis was similar to that described for **3** except using CdCl<sub>2</sub>·2H<sub>2</sub>O (0.6 mmol) instead of Zn(NO<sub>3</sub>)<sub>2</sub>·6H<sub>2</sub>O, and colorless crystals of **5** were obtained (yield: 27% based on Cd). Anal. Calcd for C<sub>112</sub>H<sub>108</sub>Cd<sub>4</sub>N<sub>28</sub>O<sub>26</sub>: C, 49.60; H, 4.01; N, 14.46. Found: C, 49.68; H, 4.05; N, 14.51. IR spectrum (cm<sup>-1</sup>): 3447 (m), 3105 (s), 1637 (s), 1513 (s), 1446 (m), 1429 (w), 1396 (w), 1356 (m), 1279 (s), 1234 (s), 1109 (s), 1090 (s), 1023 (w), 935 (m), 854 (w), 835 (m), 764 (s), 718 (s), 652 (s), 625 (m), 587 (w), 509 (w), 474 (w).

**X-ray Structural Studies.** Intensities of complexes **1** and **3–5** were collected on a Siemens SMART-CCD diffractometer with graphite monochromatic Mo K $\alpha$  radiation ( $\lambda = 0.71073$  Å) using the SMART and SAINT<sup>22</sup> programs. The structures were solved by direct methods and refined on *F*<sup>2</sup> using full-matrix least-squares

methods with SHELXTL version 5.1.<sup>23</sup> Anisotropic thermal parameters were refined for the non-hydrogen atoms. Hydrogen atoms were localized in their calculation positions and refined using a riding model.

Intensities of the complex **2** were collected on a Siemens P4 four-circle diffractometer with graphite monochromatic Mo K $\alpha$  radiation ( $\lambda = 0.71073$  Å) using the  $\omega$ -2 $\theta$  scan mode. Data were corrected for Lorentz–polarization effects during data reduction using XSCANS,<sup>24</sup> and a semiempirical absorption correction from  $\psi$ -scans was applied.<sup>25</sup>

Cavity dimensions were calculated by overlapping rigid spheres with van der Waals radii for each element: O, 1.52 Å; N, 1.55 Å; C, 1.7 Å; Cd, 2.2 Å (hydrogen atoms were omitted in all cases for simplicity). Crystallographic data and other pertinent information for **1–5** are summarized in Table 1. Selected bond lengths and bond angles are listed in Table 2. More details on the crystallographic studies as well as atomic displacement parameters are given in the Supporting Information as CIF files.

## Results and Discussion

**Crystal Structures.** [Zn(PDCO)(H<sub>2</sub>O)<sub>2</sub>]<sub>n</sub> (**1**). The structure of compound **1** crystallizes in a noncentrosymmetric space group *I*<sub>4</sub>*cd*, and the coordination geometry around zinc<sup>II</sup> center is a slightly distorted octahedron, the equatorial plane of which comprises four oxygen atoms from the carboxylate groups and *N*-oxide moieties of two different PDCO anions; two coordinated water molecules occupy the remaining apical coordination sites, as shown in Figure 1a. The Zn–O distances range from 2.036(7) to 2.121(5) Å, in the order Zn–O<sub>mean</sub>(aqua) > Zn–O<sub>mean</sub>(*N*-oxide) > Zn–O<sub>mean</sub>(carboxylate), with the O–Zn–O bond angles varying from 83.0(3) to 177.3 (3)°. The Zn–O(aqua) distance is slightly shorter than the reported value,<sup>26</sup> while the Zn–O(carboxylate) distance is within the normal range.<sup>27</sup>

(22) SMART and SAINT, Area Detector Control and Integration Software; Siemens Analytical X-ray Systems, Inc.: Madison, WI, 1996.

(23) Sheldrick, G. M. SHELXTL V5.1, Software Reference Manual; Bruker AXS, Inc.: Madison, WI, 1997.

(24) XSCANS, version 2.1; Siemens Analytical X-ray Instruments, Inc.: Madison, WI, 1994.

(25) Blessing, R. H. *Acta Crystallogr.* **1995**, *A51*, 33. Blessing, R. H. *J. Appl. Crystallogr.* **1997**, *30*, 421.

**Table 2.** Selected Bond Lengths (Å) and Bond Angles (deg) for **1–5**

Complex 1 <sup>a</sup>					
Zn(1)–O(1)	2.074(6)	Zn(1)–O(3)	2.089(7)	Zn(1)–O(1) <sup>i</sup>	2.106(7)
Zn(1)–O(2)	2.121(5)	Zn(1)–O(4)	2.036(7)	Zn(1)–O(6) <sup>i</sup>	2.047(7)
O(1)–Zn(1)–O(4)	86.7(2)	O(2)–Zn(1)–O(3)	175.2(3)	O(4)–Zn(1)–O(6) <sup>i</sup>	177.3(3)
O(1)–Zn(1)–O(1) <sup>i</sup>	174.6(2)	O(1) <sup>i</sup> –Zn(1)–O(4)	98.3(3)	O(1) <sup>i</sup> –Zn(1)–O(6) <sup>i</sup>	83.0(3)
O(1)–Zn(1)–O(6) <sup>i</sup>	91.9(2)				
Complex 2 <sup>b</sup>					
Zn(1)–O(1)	2.078(3)	Zn(1)–N(1)	2.149(3)	Zn(2)–O(8)	2.098(3)
Zn(1)–O(2)	2.149(4)	Zn(1)–N(5) <sup>i</sup>	2.156(4)	Zn(2)–O(9)	2.089(3)
Zn(1)–O(3)	2.151(3)	Zn(2)–O(6)	2.044(3)	Zn(2)–N(4)	2.194(3)
Zn(1)–O(12)	2.064(3)	Zn(2)–O(7)	2.083(3)	Zn(2)–N(2) <sup>ii</sup>	2.183(3)
O(1)–Zn(1)–O(2)	167.07(15)	O(3)–Zn(1)–O(12)	172.88(13)	O(7)–Zn(2)–O(8)	174.12(13)
O(1)–Zn(1)–O(3)	87.86(13)	N(1)–Zn(1)–N(5) <sup>i</sup>	178.47(16)	O(7)–Zn(2)–O(9)	90.90(13)
O(1)–Zn(1)–O(12)	97.37(13)	O(6)–Zn(2)–O(7)	98.20(14)	O(8)–Zn(2)–O(9)	83.41(13)
O(2)–Zn(1)–O(3)	79.27(14)	O(6)–Zn(2)–O(8)	87.54(13)	N(2) <sup>ii</sup> –Zn(2)–N(4)	173.01(19)
O(2)–Zn(1)–O(12)	95.56(15)	O(6)–Zn(2)–O(9)	170.71(13)		
Complex 3 <sup>c</sup>					
Zn(1)–O(1)	1.955(3)	Zn(1)–N(1)	1.972(3)	Zn(1)–O(4) <sup>i</sup>	2.053(3)
Zn(1)–O(3)	2.360(2)	Zn(1)–N(3)	1.988(3)		
O(1)–Zn(1)–N(1)	119.13(13)	O(3)–Zn(1)–O(4) <sup>i</sup>	164.30(11)	N(1)–Zn(1)–N(3)	125.40(13)
O(1)–Zn(1)–N(3)	112.82(14)				
Complex 4					
Zn(1)–O(1)	2.011(2)	Zn(1)–O(4)	2.049(2)	Zn(1)–N(3)	2.034(3)
Zn(1)–O(3)	2.155(2)	Zn(1)–N(1)	2.022(3)		
O(1)–Zn(1)–N(1)	136.64(11)	O(3)–Zn(1)–O(4)	168.59(9)	N(1)–Zn(1)–N(3)	108.53(11)
O(1)–Zn(1)–N(3)	112.74(11)				
Complex 5 <sup>d</sup>					
Cd(1)–O(2)	2.466(3)	Cd(1)–N(1)	2.298(4)	Cd(1)–O(4) <sup>i</sup>	2.225(3)
Cd(1)–O(3)	2.324(3)	Cd(1)–N(5)	2.292(4)	Cd(1)–N(4) <sup>ii</sup>	2.320(4)
O(2)–Cd(1)–O(3)	72.94(10)	O(3)–Cd(1)–N(5)	159.83(11)	O(4) <sup>i</sup> –Cd(1)–N(5)	106.93(12)
O(2)–Cd(1)–N(5)	88.69(11)	O(3)–Cd(1)–O(4) <sup>i</sup>	90.06(10)	N(1)–Cd(1)–N(4) <sup>ii</sup>	172.56(12)
O(2)–Cd(1)–O(4) <sup>i</sup>	161.69(10)				

<sup>a</sup> Symmetry codes: (i)  $1/2 + y, 1 - x, -1/4 + z$ . <sup>b</sup> Symmetry codes: (i)  $1 + x, y, 1 + z$ ; (ii)  $x, y, 1 + z$ . <sup>c</sup> Symmetry codes: (i)  $1 - x, 1 - y, -1/2 + z$ . <sup>d</sup> Symmetry codes: (i)  $2 - x, 1 - y, -z$ ; (ii)  $x, 1 - y, -1/2 + z$ .

Each carboxylate group is coordinated to Zn atom in a monodentate fashion. The two carboxylate groups are out of the plane of correspondingly linking pyridine rings, with the dihedral angles between them being ca. 38 and 134°, respectively, which are very distinct from those in the free PDCO, in which the carboxylate groups are found to be essentially coplanar with the pyridine rings.<sup>9</sup>

The salient structural feature of the compound **1** is it possesses a 1D helical chainlike structure with 4<sub>1</sub> helices along the *c*-axis with a pitch of 10.090 Å. The twists of PDCO<sup>2-</sup> in **1** may be responsible for the formation of the helical structure. Because left-handed and right-handed helical chains coexist in the crystal structure, the whole structure is mesomeric and does not exhibit chirality (Figure 1b). The nearest Zn···Zn separation of the adjacent helical chains is 7.635 Å. Interchain hydrogen-bonding interactions further extend the 1D helical chain to generate a 3-D framework (Table 3, Figure S1).

**[Zn<sub>2</sub>(PDCO)<sub>2</sub>(4,4'-bpy)<sub>2</sub>(H<sub>2</sub>O)<sub>2</sub>·3H<sub>2</sub>O]<sub>n</sub> (**2**). Compound **2** crystallizes in the chiral space group *P*2<sub>1</sub>, and each Zn<sup>II</sup>**

atom exhibits a distorted octahedron coordination environment formed by two oxygen atoms from a PDCO ligand, one oxygen atom from the bridging carboxylate of another PDCO, one coordinated aqua molecule occupying the basal plane, and two individual 4,4'-bpy nitrogen atoms occupying the axial sites, as illustrated in Figure 2a. The average Zn–O bond length for the *N*-oxide groups amounts to 2.123 Å, which is close to those involving the coordinated carboxylate oxygens (2.087 Å) and the water molecules (2.081 Å). The O–Zn–O bond angles range from 79.27 to 172.88°. The average Zn–N bond lengths are 2.171 Å, with the N–Zn–N bond angles varying from 173.01 to 178.47°, which is very close to the linearity. The torsion angles between the COO<sup>-</sup> group and corresponding pyridine ring range from ca. 33 to 128°. Furthermore, two pairs of pyridyl rings in the rigid 4,4'-bpy spacers are out of coplanarity, twisted by 27 and 21°, respectively. The neighboring 4,4'-bpy ligands orient almost perpendicularly to each other so that the side C–H bonds of one 4,4'-bpy are directed to the pyridyl plane of the other. A synergistic distortion effect of PDCO and 4,4'-bpy ligands leads to the formation of a chiral framework for **2**.

Compound **2** is an infinite chiral two-dimensional brick-wall-like layer structure in the *ac* plane built from achiral components, which is composed of {Zn<sub>2</sub>(PDCO)<sub>2</sub>} dimer units and 4,4'-bpy linkages, with 2<sub>1</sub> helices running along

- (26) Gable, R. W.; Hoskins, B. F.; Robson, R. *Chem. Commun.* **1990**, 1677.  
 Carlucci, L.; Ciani, G.; Gudenberg, D. W.; Proserpio, D. M.; Sironi, A. *J. Chem. Soc., Dalton Trans.* **1997**, 1801.  
 (27) MacDonald, J. C.; Dorrestein, P. C.; Pilley, M. M.; Foote, M. M.; Lundburg, J. L.; Henning, R. W.; Schultz, A. J.; Manson, J. L. *J. Am. Chem. Soc.* **2000**, *122*, 11692. Zheng, S. L.; Yang, J. H.; Yu, X. L.; Chen, X. M.; Wong, W. T. *Inorg. Chem.* **2004**, *43*, 830.

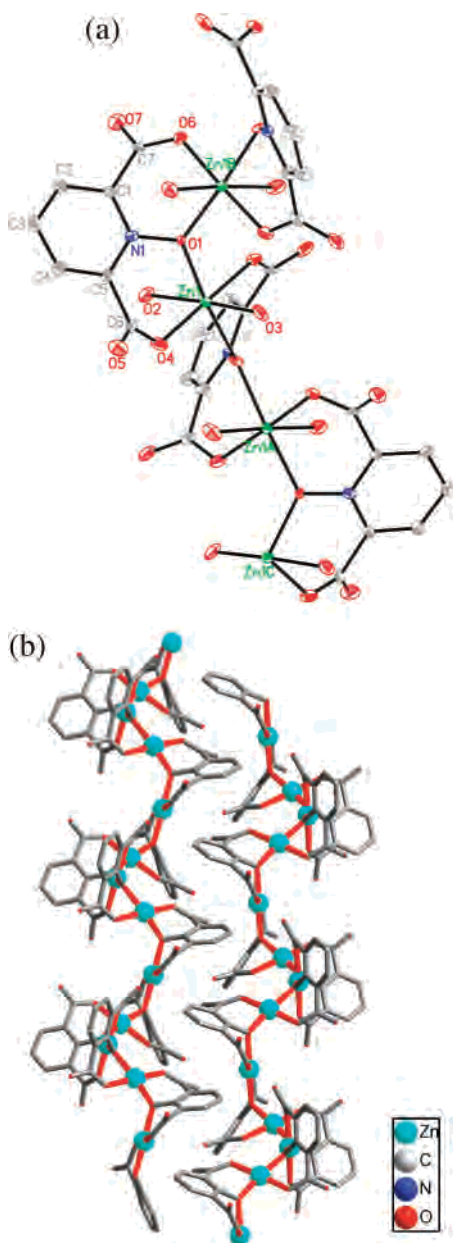


**Figure 1.** (a) ORTEP view of **1** with hydrogen atoms omitted for clarity. Thermal ellipsoids are drawn at the 30% probability level. (b) Stereoview of adjacent two helices for **1**. Hydrogen atoms and coordinated water molecules have been omitted for clarity.

the *c*-axis (Figure 2b,c). All the helices lie along the same direction and exhibit the same chirality. Each rectangular grid of the brick-wall-like layer is organized by four PDCO ligands acting as the two shorter edges (5.551 Å), four 4,4'-bpy groups acting as the two longer edges (22.951 Å), four Zn atoms representing the four vertexes, and two more Zn atoms serving as the midpoints of the longer edges. The free water molecules are included between the layers, and the layers are stacked in an –ABAB– sequence along the *b* axis with strong interlayer hydrogen-bond interactions by the coordinated and free water molecules linking the carboxylic acid moieties, thus leading to the construction of a three-dimensional host–guest network (Table 3, Figure S2).

[Zn(PDCO)(bix)]<sub>n</sub> (**3**) and [Zn(PDCO)(bbi)·0.5H<sub>2</sub>O]<sub>n</sub> (**4**). For compounds **3** and **4**, though the bridging ligands

**Table 3.** Distances (Å) and Angles (deg) of Hydrogen Bonding for Complexes **1** and **2**

D–H···A	<i>d</i> (D···A)	–D–H···A
Compound <b>1</b> <sup>a</sup>		
O(2)–H(2A)···N(1) <sup>i</sup>	2.921(9)	122.00
O(2)–H(2B)···O(7) <sup>ii</sup>	2.862(9)	122.00
O(3)–H(3A)···O(6) <sup>iii</sup>	2.676(10)	139.00
O(3)–H(3B)···O(4) <sup>iv</sup>	2.778(10)	149.00
C(2)–H(2)···O(7) <sup>v</sup>	3.320(11)	143.00
C(3)–H(3)···O(5) <sup>vi</sup>	3.369(12)	166.00
Compound <b>2</b> <sup>b</sup>		
O(1)–H(1B)···O(9) <sup>i</sup>	2.693(5)	120.00
O(7)–H(7A)···O(3) <sup>ii</sup>	2.767(5)	136.00
O(7)–H(7B)···O(5)	2.784(5)	135.00
O(13)–H(13A)···O(15) <sup>iii</sup>	2.835(3)	157.00
O(13)–H(13B)···O(5)	2.905(4)	116.00
O(14)–H(14A)···O(11) <sup>iv</sup>	2.945(5)	128.00
O(15)–H(15A)···O(1) <sup>ii</sup>	2.792(4)	158.00
O(15)–H(15B)···O(11) <sup>ii</sup>	2.792(4)	157.00
C(5)–H(5)···O(6)	3.007(6)	123.00
C(5)–H(5)···O(8)	3.450(6)	161.00
C(10)–H(10)···O(12) <sup>vi</sup>	3.158(5)	148.00
C(19)–H(19)···O(14)	3.422(6)	168.00
C(31)–H(31)···O(5) <sup>vii</sup>	3.248(6)	134.00

<sup>a</sup> Symmetry codes: (i)  $1/2 + y, 1 - x, -1/4 + z$ ; (ii)  $2 - x, y, -1/2 + z$ ; (iii)  $3/2 - x, 1/2 - y, -1/2 + z$ ; (iv)  $1 - y, -1/2 + x, 1/4 + z$ ; (v)  $2 - x, 1 - y, z$ ; (vi)  $1/2 + y, x, 1/4 + z$ . <sup>b</sup> Symmetry codes: (i)  $1 + x, y, z$ ; (ii)  $-1 + x, y, z$ ; (iii)  $1 - x, -1/2 + y, 1 - z$ ; (iv)  $2 - x, -1/2 + y, 1 - z$ ; (v)  $1 - x, -1/2 + y, 1 - z$ ; (vi)  $x, y, -1 + z$ ; (vii)  $2 - x, 1/2 + y, 2 - z$ .

are different and are more flexible than 4,4'-bpy, in addition, bbi is more variable than bix; both structures have only one repeating metallic structural motif, with each crystallographically unique Zn<sup>II</sup> metal center in a less-common distorted trigonal bipyramidal coordination sphere, {ZnN<sub>2</sub>O<sub>3</sub>}, which is defined by two oxygen donors respectively from a carboxylate and a *N*-oxide group of two distinct PDCO's in the axial positions while the equatorial positions are furnished by two different bix (or bbi) nitrogen donors and one carboxylate oxygen donor, as displayed in Figure 3a and Figure 4a.

In **3**, the Zn–O bond lengths for the coordinated carboxylate groups range from 1.955(3) to 2.053(3) Å, which are obviously shorter than the Zn–O(*N*-oxide) distance of 2.360(2) Å, and the Zn–N bond lengths are 1.972(3) and 1.988(3) Å, respectively. Two carboxylate groups form dihedral angles of ca. 66 and 31° with the correspondingly pyridine rings plane. The bix ligands adopt a *cis* conformation, with the dihedral angles between the imidazole rings of ca. 46°, while the distortion angles between the imidazole rings and the average plane of phenyl group are ca. 103 and 79°, respectively.

In **4**, the Zn–O bond lengths range between 2.011(2) and 2.155(2) Å. The Zn–N bond lengths are 2.022(3) and 2.034(3) Å, which are slightly longer with respect to those involved in **3**. The distortion angles between COO<sup>–</sup> groups and pyridine rings range from ca. 32 to 134°. The bbi ligand has an extended geometry in which the N–(CH<sub>2</sub>)<sub>4</sub>–N chain has an all *anti* geometry, and the planes of the imidazole rings are inclined by ca. 62° to each other.

For both compounds, the fully deprotonated PDCO<sup>2–</sup> anions act as effective tridentate bridging ligands linking the Zn metal centers by monodentate carboxylate and *N*-oxide groups, imposing separations of Zn···Zn<sup>i</sup> 6.008 Å and

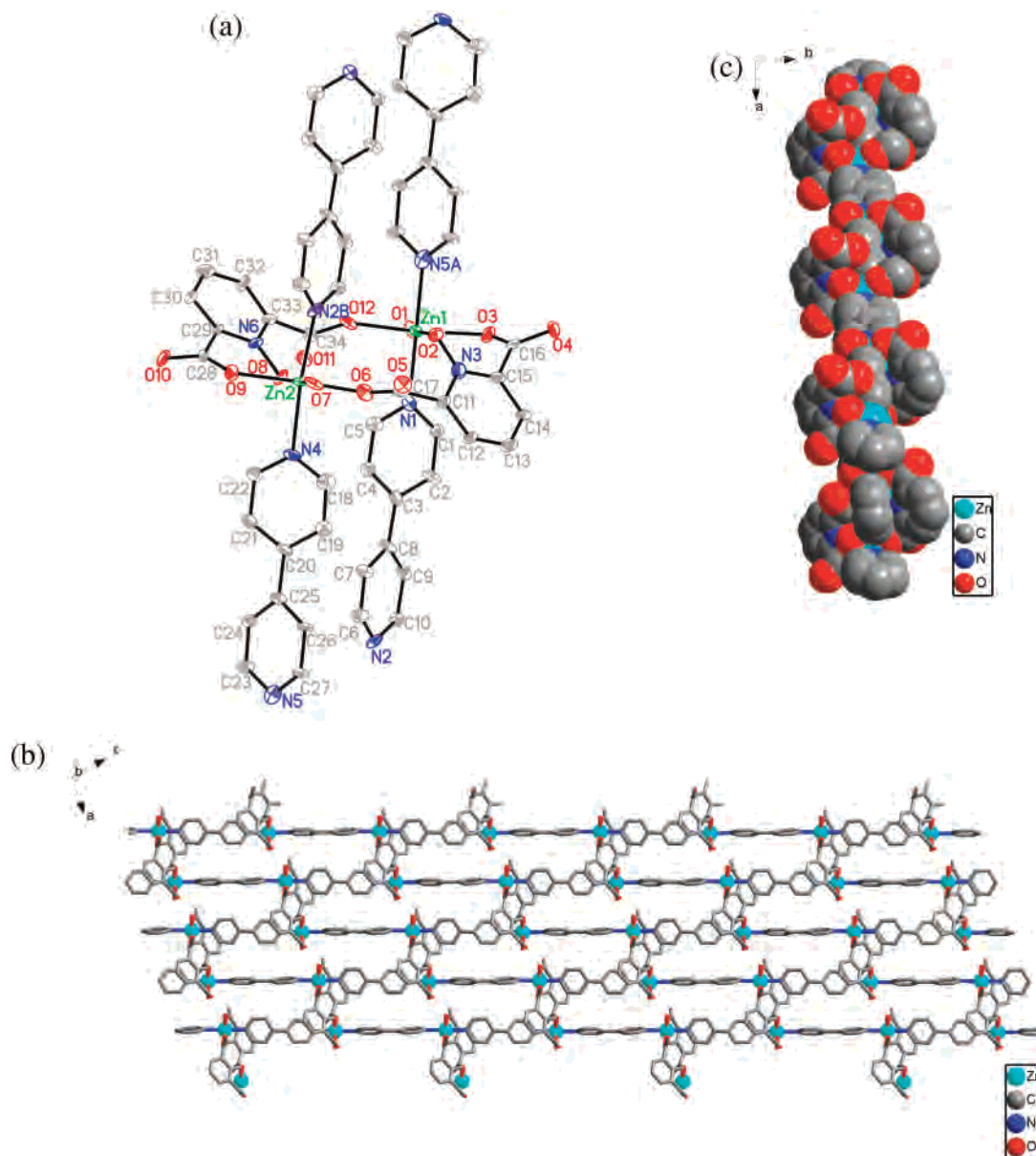


**Figure 2.** (a) ORTEP view of **2** with hydrogen atoms and free water molecules omitted for clarity (30% probability ellipsoids). (b) View toward the *ac* plane of the 2D brick-wall-like framework. (c) Space-filling model for a helical stereoview of **2**.

$\text{Zn}^{\cdots}\text{Zn}^{\text{II}}$  6.499 Å for **3** and **4**, respectively [symmetry code: (i)  $1 - x, 1 - y, -1/2 + z$ ; (ii)  $-1/2 + x, y, 3/2 - z$ ]. All the bidentate bix or bbi molecules establish a physical bridge between Zn atoms, imposing  $\text{Zn}^{\cdots}\text{Zn}^{\text{III}}$  separations of 10.475 Å for **3** and  $\text{Zn}^{\cdots}\text{Zn}^{\text{IV}}$  separations of 13.446 Å for **4** [symmetry code: (iii)  $1 - x, 1 - y, 1/2 + z$ ; (iv)  $-x, 1/2 + y, 3/2 - z$ ].

It is noteworthy that the repetition of the  $\{\text{ZnN}_2\text{O}_3\}$  metallic structural motif of **3** generates an infinite 2D herringbone architecture extended in the *ac* plane of the unit cell (Figure 3b). The resulting 2D structure is cross-linked by weaker hydrogen-bond interactions between C–H groups from a bix ligand and uncoordinated carboxylate or *N*-oxide oxygen atoms, thus producing a 3D framework (Table 4, Figure S3).

Interestingly, there is a 34-membered metalocycle in the 2D layer developed in the *ab* plane for **4**, which is composed of two PDCO, two bbi units, and four Zn atoms acting as

connecting nodes, also distributed in the herringbone manner (Figure 4b). Lattice water molecules are also included between the layers, and the relatively weaker  $\text{O}_{\text{water}}-\text{H}^{\cdots}\text{N}$  and  $\text{C}-\text{H}^{\cdots}\text{O}_{\text{carboxylate}}$  hydrogen bonds complete the final 3D architecture (Table 4, Figure S4).

Complexes **3** and **4** are similar in their coordination mode and network structure. Both compounds crystallize in the orthorhombic crystal system; however, noncentrosymmetric space group *Pca*2<sub>1</sub> for **3** and centrosymmetric space group *Pbca* for **4** are observed. The difference may originate from the different conformations of the bix and bbi ligands in the structures.<sup>28</sup>

$[\text{Cd}(\text{PDCO})(\text{bix})_{1.5}\cdot 1.5\text{H}_2\text{O}]_n$  (**5**). Though the ligands are the same as in **3**, the structure of **5** is significantly different from **3** because of its different metal centers. It is a most

(28) Fan, J.; Sun, W. Y.; Okamura, T.-a.; Tang, W. X.; Ueyama, N. *Inorg. Chem.* **2003**, *42*, 3168. Fan, J.; Sui, B.; Okamura, T.-a.; Sun, W. Y.; Tang, W. X.; Ueyama, N. *J. Chem. Soc., Dalton Trans.* **2002**, 3868.

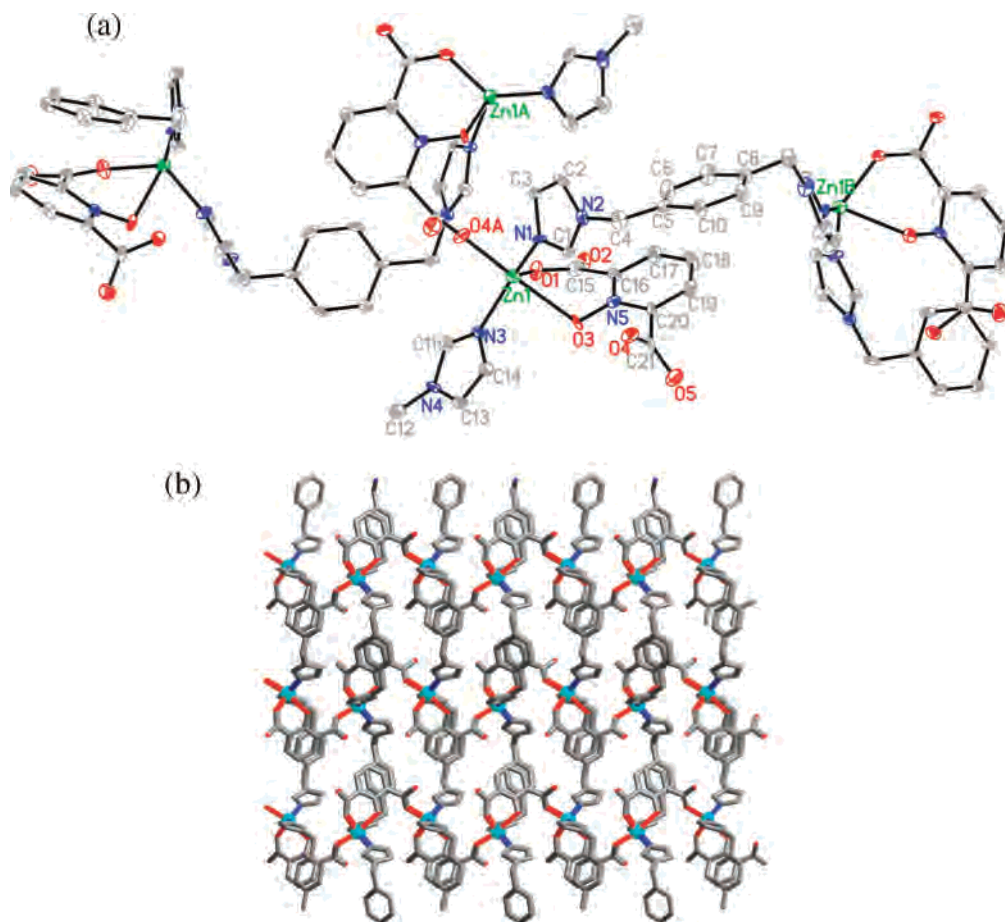


**Figure 3.** (a) ORTEP view of **3** with hydrogen atoms omitted for clarity. (b) View toward the *ac* plane of the 2D herringbone architecture.

remarkable and unique three-dimensional coordination polymer where each  $\text{Cd}^{\text{II}}$  atom exhibits a distorted hexahedral configuration with a  $\text{N}_3\text{O}_3$  donor set, as depicted in Figure 5. The Cd atom is coordinated by three individual bix nitrogen atoms with Cd–N bond distances varying from 2.292(4) to 2.320(4) Å. Three additional positions are occupied by oxygen atoms from two individual PDCO groups with Cd–O bond distances varying from 2.225(3) to 2.466(3) Å. These bond lengths are comparable to those reported values.<sup>29,30</sup> The  $\text{COO}^-$  groups deviate from the plane of correspondingly pyridine rings with the dihedral angles between them being ca. 57 and 80°. For the bix ligand containing N1, two terminal imidazole groups are in *cis* conformation and the dihedral angles between the imidazole ring planes and the least-squares plane of the phenyl group are 79 and 110°, respectively, while the two imidazole groups twist by 45°. However, in the case of the bix containing N5, residing at crystallographic inversion center, two terminal imidazole groups assume a *trans* conformation and have their planes steeply inclined, by 74°, to the average plane of the phenyl group.

It is worth noting that the structure is composed of a one-dimensional wavelike architecture with a period equal to the

*c* axis, which is constructed from *cis*-bix and PDCO ligands, and the 1D structure is further stacked along the *a* and *b* directions, with the bidentate *trans*-bix spacers occupying the void spaces, thus leading to the formation of a three-dimensional porous framework. The crystal structure of **5** contains channels in two directions, both distributed in a rectangular grid fashion, which are filled by the 3 crystallographically unique uncoordinated water molecules involved in C–H···O and O–H···O hydrogen bonds (Table 4). The most prominent cavities are ca. 10.4 × 9.0 Å in cross section and run along the *c* axis; other rectangular-shaped, but smaller, channels with cross section of ca. 7.3 × 9.0 Å are parallel to the *b* direction, as indicated in Figure 6.

Interestingly, the presence of large free voids in the  $[\text{Cd}(\text{PDCO})(\text{bix})_{1.5} \cdot 1.5\text{H}_2\text{O}]_n$  single framework result in the formation of interpenetrations. The channels of  $[\text{Cd}(\text{PDCO})(\text{bix})_{1.5} \cdot 1.5\text{H}_2\text{O}]_n$  are filled by another identical framework in a typical 2-fold interpenetration fashion, displaced by the usual half of the length of the unit, as illustrated in Figure 7. As a result, **5** exhibits a 2-fold self-interpenetration 3D framework related by symmetry. Usually, the coexistence of both *syn* and *anti* conformations of bix leads to an unusual interpenetrating network.<sup>31</sup> Although many entangled struc-

(29) Tao, J.; Tong, M. L.; Chen, X. M. *J. Chem. Soc., Dalton Trans.* **2000**, 3669.

(30) Fujita, M.; Aoyagi, M.; Ogura, K. *Bull. Chem. Soc. Jpn.* **1998**, *71*, 1799.

(31) Abrahams, B. F.; Hoskins, B. F.; Robson, R.; Slizys, D. A. *CrystEngComm* **2002**, *4*, 478. Carlucci, L.; Ciani, G.; Proserpio, D. M.; Spadacini, L. *CrystEngComm* **2004**, *6*, 96. Gao, E. Q.; Xu, Y. X.; Yan, C. H. *CrystEngComm* **2004**, *6*, 298.

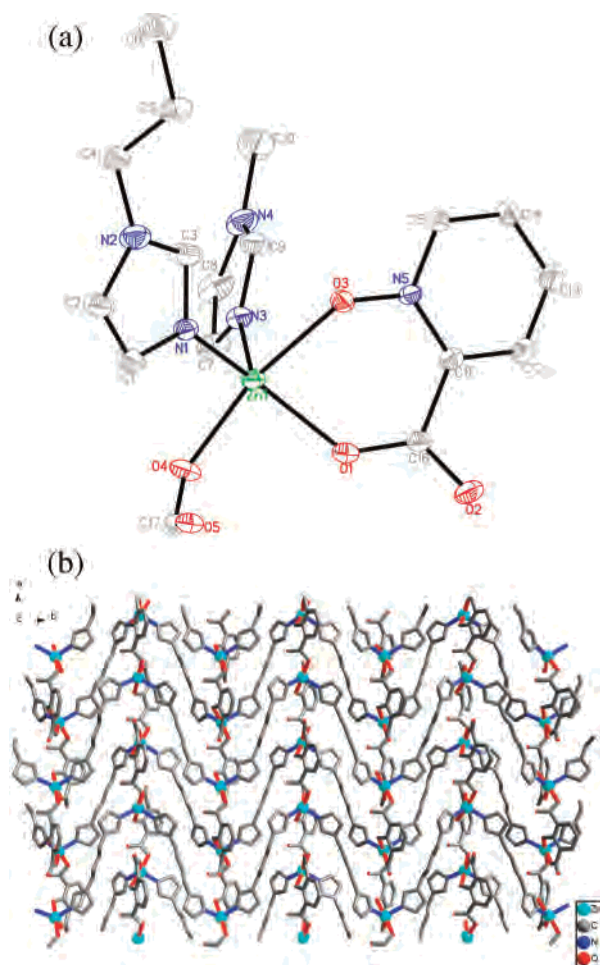


**Figure 4.** (a) ORTEP view of **4** with hydrogen atoms and free water molecules omitted for clarity. (b) View toward the *ab* plane of the 2D herringbone architecture.

**Table 4.** Distances (Å) and Angles (deg) of Hydrogen Bonding for Complexes **3–5**

D–H...A	<i>d</i> (D...A)	–D–H...A
Compound <b>3</b> <sup>a</sup>		
C(1)–H(1)···O(4)	3.099(4)	154.00
C(4)–H(4B)···O(3) <sup>i</sup>	3.362(6)	142.00
C(12)–H(12A)···O(2) <sup>ii</sup>	3.192(6)	141.00
C(18)–H(18)···O(5) <sup>iii</sup>	3.196(6)	125.00
Compound <b>4</b> <sup>b</sup>		
O(6)–H(6F)···N(5) <sup>i</sup>	3.338(14)	161.00
C(1)–H(1)···O(5)	3.096(5)	127.00
C(8)–H(8)···O(5) <sup>ii</sup>	3.105(6)	146.00
C(14)–H(14)···O(2) <sup>iii</sup>	3.126(5)	133.00
Compound <b>5</b> <sup>c</sup>		
O(6)–H(6B)···O(7)	3.233(11)	138.00
O(7)–H(7A)···O(8)	3.135(10)	150.00
O(7)–H(7B)···O(1) <sup>i</sup>	2.776(7)	113.00
O(8)–H(8A)···O(1) <sup>ii</sup>	2.967(9)	116.00
C(1)–H(1)···O(4) <sup>iii</sup>	3.062(5)	118.00
C(11)–H(11A)···O(3) <sup>iv</sup>	3.324(6)	159.00
C(15)–H(15)···O(7) <sup>ii</sup>	3.169(7)	150.00

<sup>a</sup> Symmetry codes: (i)  $x, 1 + y, z$ ; (ii)  $1 - x, -y, 1/2 + z$ ; (iii)  $3/2 - x, y, -1/2 + z$ . <sup>b</sup> Symmetry codes: (i)  $-1/2 + x, y, 3/2 - z$ ; (ii)  $3/2 - x, 1/2 + y, z$ ; (iii)  $-1/2 + x, 1/2 - y, 2 - z$ . <sup>c</sup> Symmetry codes: (i)  $x, y, 1 + z$ ; (ii)  $1 - x, y, 1/2 - z$ ; (iii)  $2 - x, 1 - y, -z$ ; (iv)  $x, -y, 1/2 + z$ .

tures have been reported, those constructed by mixed ligands are rather few.<sup>32</sup>

Apparently, the formation of MOFs depends on the combination of several factors, such as the coordination geometry of metal ions, the nature of ligands,<sup>33</sup> the ratio between metal salt and ligand,<sup>34</sup> and reaction conditions such as solvent system and templates. In this study, the hydrothermal reaction of PDCO and  $\text{Zn}(\text{NO}_3)_2$  produces **1**, which generates a 1D helical chainlike structure. When the neutral bridging ligands 4,4'-bpy, bix, and bbi are introduced into the reaction system, compounds **2–4** give rise to a diversity of frameworks: **2** is an infinite chiral two-dimensional brick-wall-like layer structure; both **3** and **4** exhibit infinite 2D herringbone architectures. Complexes **1–4** all form a 3D array considering the hydrogen-bonding interactions. Most interestingly, the hydrothermal reaction of PDCO and bix in the presence of  $\text{CdCl}_2 \cdot 2\text{H}_2\text{O}$  affords **5**, which is a 2-fold interpenetration three-dimensional coordination polymer.

In these five compounds, all the carboxyl groups adopt a monodentate coordination mode to connect metal atoms. This type of coordination fashion is similar to that for  $\{\text{Ln}_2(\text{pdc})_3 \cdot 3\text{H}_2\text{O}\}$ <sup>35</sup> and  $\{[\text{Ln}(\text{pdc})_3\text{Mn}_{1.5}(\text{H}_2\text{O})_3] \cdot n\text{H}_2\text{O}\}$  (pdc = pyridine-2,6-dicarboxylic acid).<sup>36</sup> For **2**, the 4,4'-bpy ligand is rigid, which may facilitate the formation of a homohanded helix, hence, giving rising to the chiral framework. The bix ligand is highly variable, which makes it adaptable to different polymeric coordination structures. It assumes a *cis* conformation in **3** vs both *cis* and *trans* conformations in the case of **5**, according to the different geometric needs of metal ions. Consequently, the versatile conformation of bix ligand intricately influences the crystal packing. Although bbi is more variable than bix, it only exhibits an *anti* conformation in **4** and the other previously reported compounds containing bbi.<sup>37</sup> Indeed, due to a different degree in rigidity/flexibility of the neutral bridging ligands and in atom radius of metal centers, systematic variations in dimensionality (1D  $\rightarrow$  2D  $\rightarrow$  3D) of the coordination polymer frameworks can be obtained, indicating ligand-directed and metal-directed synthesis.

**Thermal Analysis.** For **1**, the weight loss of 12.82% below 207 °C (calcd 12.74%) corresponds to the loss of two coordinated water molecules/formula. Then the compound begins to decompose. For **2**, the weight loss attributed to the gradual release of free aqua ligands is observed below 80 °C (obsd 5.66%, calcd 6.03%). The second loss corresponding to the release of almost all coordinated water molecules is detected between 80 and 160 °C (obsd 4.29%, calcd 4.02%). Two consecutive decompositions suggest the

- (32) Paz, F. A. A.; Klinowski J. *Inorg. Chem.* **2004**, *43*, 3882. Paz, F. A. A.; Klinowski, J. *Inorg. Chem.* **2004**, *43*, 3948.  
 (33) Hirsch, K. A.; Wilson, S R.; Moore, J. S. *Inorg. Chem.* **1997**, *36*, 2960. Bu, X. H.; Chen, W.; Lu, S. L.; Zhang, R. H.; Liao, D. Z.; Bu, W. M.; Shionoya, M.; Brisse, F.; Ribas, J. *Angew. Chem., Int. Ed.* **2001**, *40*, 3201. Kitaura, R.; Fujimoto, K.; Noro, S.; Kondo, M.; Kitagawa, S. *Angew. Chem., Int. Ed.* **2002**, *41*, 133. Kitaura, R.; Seki, K.; Akiyama, G.; Kitagawa, S. *Angew. Chem., Int. Ed.* **2003**, *42*, 428.  
 (34) Carlucci, L.; Ciani, G.; Gudenberg, D. W.; Proserpio, D. M.; Sironi, A. *Chem. Commun.* **1997**, 631.  
 (35) Ghosh, S. K.; Bharadwaj, P. K. *Inorg. Chem.* **2004**, *43*, 2293.  
 (36) Zhao, B.; Cheng, P.; Dai, Y.; Cheng, C.; Liao, D. Z.; Yan, S. P.; Jiang, Z. H.; Wang, G. L. *Angew. Chem., Int. Ed.* **2003**, *42*, 934.  
 (37) Ma, J. F.; Yang, J.; Zheng, G. L.; Li, L.; Zhang, Y. M.; Li, F. F.; Liu, J. F. *Polyhedron* **2004**, *23*, 553.



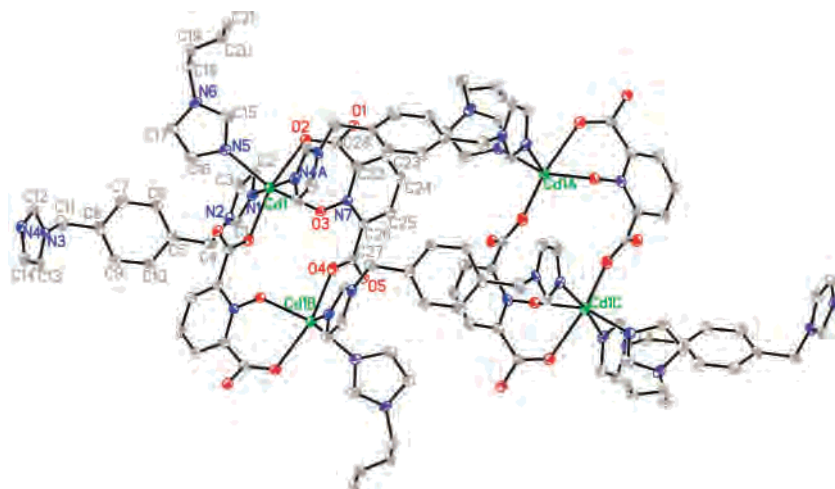


**Figure 5.** ORTEP view of **5** with hydrogen atoms and water molecules omitted for clarity.

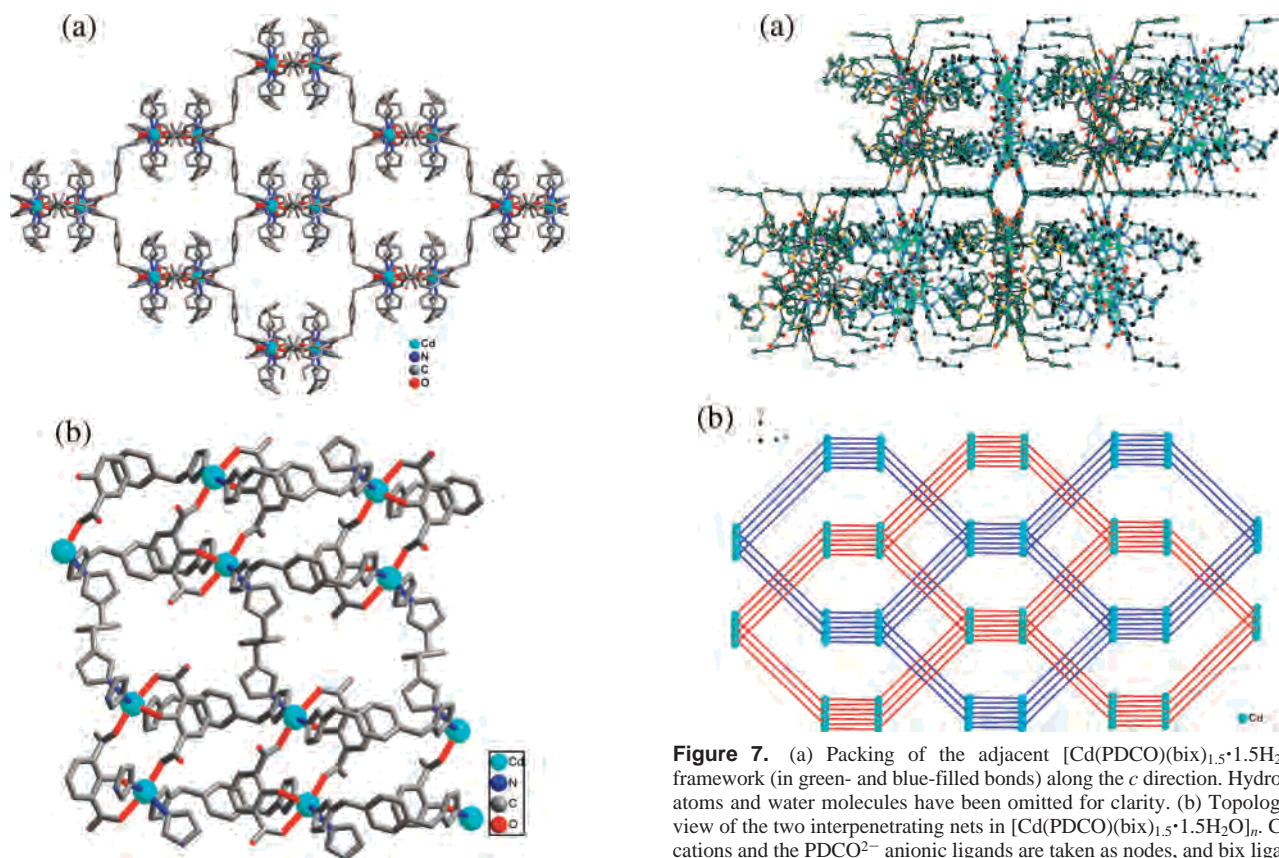


**Figure 6.** Projections along the (a) *c* direction and (b) *b* direction of the 3D  $[\text{Cd}(\text{PDCO})(\text{bix})_{1.5} \cdot 1.5\text{H}_2\text{O}]_n$  framework in **5** showing the cavities. Hydrogen atoms and water molecules have been omitted for clarity, and cross sections have been calculated on the basis of van der Waals radii.

total destruction of the framework by the oxidation of the organic component, leading to the formation of the stoichiometric amount of zinc oxide as the residues (obsd 18.68%, calcd 18.18%). Compounds **3** and **4** are stable up to 233 and 220 °C, respectively, where the framework structures begin to collapse. A plateau region is observed for **4** from 520 to 800 °C and a brown residue of ZnO (obsd 18.67%, calcd 18.26%) remained. For **5**, the first weight loss of 4.07% below 250 °C is assigned to the liberation of free water molecules, which is in agreement with the calculated value

**Figure 7.** (a) Packing of the adjacent  $[\text{Cd}(\text{PDCO})(\text{bix})_{1.5} \cdot 1.5\text{H}_2\text{O}]_n$  framework (in green- and blue-filled bonds) along the *c* direction. Hydrogen atoms and water molecules have been omitted for clarity. (b) Topological view of the two interpenetrating nets in  $[\text{Cd}(\text{PDCO})(\text{bix})_{1.5} \cdot 1.5\text{H}_2\text{O}]_n$ .  $\text{Cd}^{2+}$  cations and the  $\text{PDCO}^{2-}$  anionic ligands are taken as nodes, and *bix* ligands are substituted by a connection between metals.

(3.98%). The second weight loss occurs in the range 250–494 °C, which is attributed to the elimination of the PDCO ligand (obsd 26.74%, calcd 26.70%). The guest molecules are difficult to remove from the host molecules due to the existence of strong hydrogen bonds between the host and guest molecules.

Guest water molecules are removed by heating **2** and **5** at 80 and 250 °C for 2 h under  $\text{N}_2$ , respectively. Powder X-ray diffraction study of **2** and **5** before and after water expulsion shows only minor changes in the diffraction patterns, which indicate the chiral MOFs of **2** and 3D 2-fold interpenetration MOFs of **5** are intact after removal of the guest water molecule.

**Photoluminescence Properties.** The emission spectra of complexes **1–5** in the solid state at room temperature are investigated. Excitation at 342 nm leads to stronger blue-fluorescent emission bands at 417 nm for **1**, 447 nm for **4**, and 418 nm for **5** while weaker blue-fluorescent emission bands are observed at 420 nm for **2** and 458 nm for **3**, respectively, under the same conditions. These emissions are neither metal-to-ligand charge transfer (MLCT) nor ligand-to-metal transfer (LMCT) in nature since the  $Zn^{2+}$  or  $Cd^{2+}$  ions are difficult to oxidize or to reduce due to their  $d^{10}$  configuration which can probably be assigned to the intraligand ( $\pi-\pi^*$ ) fluorescent emission because similar emissions are observed for the free PDCO at 416 nm. It is clear that bathochromic shift of emission occurs in **3** and **4**, compared with other compounds, which is probably due to the differences of ligands and coordination environment around central metal ions, because photoluminescence behavior is closely associated with the local environments around metal ions.<sup>38</sup> Complexes **1**, **4**, and **5** may be suitable as excellent candidates of blue-fluorescent materials, since they are highly thermally stable and insoluble in common solvents.<sup>39</sup>

**SHG Measurement.** Given that **1–3** all crystallize in a noncentrosymmetric space group, preliminary SHG responses of these complexes are estimated by measuring a powder sample (ca. 80–120  $\mu m$  in diameter, Kurtz powder test),<sup>40</sup> relative to urea. The SHG efficiency of **1–3** is estimated to be approximately 0.3, 0.3, and 0.9 times of that of urea, respectively, which confirm their noncentric frameworks. These SHG properties reflect the molecular arrangements in the crystals. Compound **3** displays higher SHG efficiency compared with **1** and **2**, and the reason may be attributed to the herringbone arrangement in the lattice of **3**, which induces the large charge-transfer interaction to result in the higher SHG efficiency.<sup>41</sup> Similar phenomena have been observed in the cocrystals of 2-amino-3-nitropyridine or 2-amino-5-nitropyridine with achiral benzenesulfonic acids.<sup>42</sup> Thus, **3**

appears to be a good candidate of novel hybrid inorganic–organic NLO materials. **1–3** display different NLO properties owing to them having different architectures. It is obvious that the NLO properties of coordination polymers can be altered through structural manipulation.

## Conclusion

In summary, five novel polymers with different architectures,  $[Zn(PDCO)(H_2O)_2]_n$  (**1**),  $[Zn_2(PDCO)_2(4,4'-bpy)_2(H_2O)_2 \cdot 3H_2O]_n$  (**2**),  $[Zn(PDCO)(bix)]_n$  (**3**),  $[Zn(PDCO)(bbi) \cdot 0.5H_2O]_n$  (**4**), and  $[Cd(PDCO)(bix)_{1.5} \cdot 1.5H_2O]_n$  (**5**), were constructed from the PDCO ligand, in the presence of different N-heterocycles used as spacers under mild hydrothermal conditions. For the first time, pyridine dicarboxylic acid *N*-oxide has been introduced into the  $d^{10}$  metal coordination polymer system. This study not only demonstrates that the nature of ligands and the geometric needs of metal atoms play an important role in the crystal packing of MOFs but also illustrates that the hydrogen bonds affect the formation of the supramolecular architecture. In addition, complexes **1**, **4**, and **5** may be excellent candidates for blue-fluorescent materials and **3** appears to be a good candidate of novel hybrid inorganic–organic NLO materials.

**Acknowledgment.** We thank the National Natural Science Foundation of China (Grant No.20490218), Jiangsu Science & Technology Department, and the Center of Analysis and Determination of Nanjing University for the financial support.

**Supporting Information Available:** X-ray crystallographic files in CIF format, figures of crystal packing, TG curves, photoluminescent spectra, and an X-ray powder diffraction diagram. This material is available free of charge via the Internet at <http://pubs.acs.org>.

IC0509985

(38) Fu, Z. Y.; Wu, X. T.; Dai, J. C.; Hu, S. M.; Du, W. X.; Zhang, H. H.; Sun, R. Q. *Eur. J. Inorg. Chem.* **2002**, 2730.

(39) Tao, J.; Tong, M. L.; Shi, J. X.; Chen, X. M.; Ng, S. W. *Chem. Commun.* **2000**, 2043.

(40) Kurtz, S. K.; Perry, T. T. *J. Appl. Phys.* **1968**, 39, 3798.

(41) Masse, R.; Zyss, J. *Mol. Eng.* **1991**, 1, 141. Kotler, Z.; Hierle, R.; Josse, D.; Masse, R. *J. Opt. Soc. Am.* **1992**, B9, 534.

(42) Koshima, H.; Miyamoto, H.; Yagi, I.; Uosaki, K. *Cryst. Growth Des.* **2004**, 4, 807. Koshima, H.; Hamada, M.; Yagi, I.; Uosaki, K. *Cryst. Growth Des.* **2001**, 1, 467.